ARTICLE

Check for updates

Arctic deep-water anoxia and its potential role for ocean carbon sink during glacial periods

Kwangchul Jang [1], Kyung Sik Woo [1,2 ✉], Jin-Kyoung Kim[3] & Seung-Il Nam [1 ✉]

Deep water freshening beneath pan-Arctic ice shelves has recently been proposed based on the absence of excess thorium in glacial Arctic sediments. This profound proposal requires scrutiny of Arctic paleohydrology during past glacial periods. Here, we present structural and geochemical results of inorganic authigenic carbonates in deep-sea glacimarine sediments from the Mendeleev Ridge, western Arctic Ocean over the last 76 kyr. Our results suggest that Polar Deep Water in the western Arctic became brackish and anoxic during stadial periods. We argue that sediment-laden hyperpycnal meltwater discharged from paleo-ice sheets filled much of the water column depending upon the density, substantially reducing the salinity and oxygen content of the Polar Deep Water. Our findings suggest that this phenomenon was more extreme in the western Arctic Ocean and may point to the potential role of the western Arctic Ocean as an additional carbon reservoir in the global carbon cycle across glacial-interglacial cycles.

[1] Division of Glacial Environment Research, Korea Polar Research Institute, Incheon 21990, South Korea. [2] Department of Geology, Kangwon National University, Chuncheon, Gangwondo 24341, South Korea. [3] Radpion Incorporation, Daejeon 34014, South Korea. ✉email: happyman369@naver.com; sinam@kopri.re.kr

Glacial periods are characterised by lower atmospheric CO_2 concentrations than today, which cause a substantial fraction of global cooling[1]. A large proportion of the diminished carbon from the atmosphere during glacial periods was stored in deep oceans, the largest CO_2 reservoir[2]. In this regard, the Southern Ocean has been identified as a major CO_2 sink during glacial periods based on the evidence for strong ocean stratification[2] that led to oxygen depletion[3]. On the other hand, the role of the Arctic Ocean in glacial CO_2 drawdown has not been considered. Despite dysoxic bottom waters being suggested as a possible cause for the absence of Mn in glacial sediments[4], the prevailing paradigm is that the Arctic Ocean was mostly oxygenated during the late Quaternary.

However, the recent suggestion of the Arctic Ocean being a freshwater filled basin during marine isotope stages (MIS) 6 and 4 (ref. [5]) triggered the revaluation of these past concepts[6,7]. The deep Arctic Ocean is generally saline and well-oxygenated at present[8], in which the brine formed in coastal polynyas plays a crucial role in deep ventilation[9] (Supplementary Note 1). On the other hand, glacial Arctic hydrology such as salinity[5–7] and oxygenation[10–12] is still under debate because of controversial geochemical evidence (Supplementary Note 2). Given that foraminifera records are discontinuous and tend not to be preserved during unfavourable intervals for their survival such as oceanic freshening (e.g., ref. [5]) and anoxia, it is necessary to develop and apply alternative proxies and archives to reconcile inconsistencies between the paleoceanographic reconstructions in the Arctic Ocean.

Here, we provide an almost continuous record of the authigenic carbonates in glacimarine pelagic sediments at site PS72/410-1 from the Mendeleev Ridge in the western Arctic Ocean since the last glacial period (Fig. 1). The in-situ formed authigenic carbonates and their textural and geochemical properties provide direct information on the origin and associated prevailing oceanographic conditions for the Polar Deep Water (PDW) (Supplementary Note 3). The results indicate that brackish and anoxic PDW, at least in the western Arctic, predominantly prevailed during stadial periods such as MIS 4 to early 3 (hereafter MIS 4-3) and MIS 2, probably due to oxygen-depleted meltwater intrusion. This raises important questions on the role of the Arctic Ocean as an atmospheric carbon regulator.

Results and Discussion
Authigenic calcites as an archive of the PDW. Authigenic carbonates are found throughout the sediment core (up to a depth of 39 cm), except for a few intervals (21–23 and 32–35 cm). Two intervals at core depths of 4–6 cm and 25–30 cm contain relatively higher contents. Carbonate crystals consist of calcite (and Mg-calcite) and aragonite, and various growth textures indicate their inorganic origin. Calcite (and Mg-calcite) crystals show two types of growth habits: either bundles of platy calcite crystals (foliated ultrastructure) or individual calcite crystals. Bundles of platy calcite crystals sometimes show the overall spherical growth pattern of each bundle (Fig. 2a). Bundles of calcite plates invariably comprise a stack of thin folia with isosceles triangle shapes (Fig. 2b and c). Individual calcite crystals show equant, bladed to fibrous textures and occasional aggregates of several crystals. Aragonite crystals mostly display fibrous textures, which are composed of needle-shaped crystals. Square-ended terminations of each crystal confirm its aragonite mineralogy[13]. Aragonite needles either show spherulitic growth fabric (Fig. 2d) or randomly oriented fabric (Fig. 2e). Although rare, two stages of aragonite growth after calcite are present (Fig. 2f).

Authigenic calcites occur in core-top sediment (<1 cm). This implies that the fluid at the sediment-water interface has been saturated with respect to calcite. Indeed, Arctic seawater is saturated with respect to calcite and aragonite to some extent at present, most likely resulting from low sedimentation and organic respiration rates[14]. Considering lower to similar sedimentation[15] and total organic carbon contents at site PS72/410-1 during the last glacial period (Supplementary Fig. 1), the calcite saturation of ambient seawater at site PS72/410-1 could have been persistent over the last 76 kyr, leading to the continuous precipitation of authigenic calcites at the sediment-water interface. This allows the continuous record of the PDW signatures, except for two absent intervals. On the other hand, the authigenic aragonites are found from slightly deeper depths (>1 cm) and often occur as an overgrowth on calcites, implying possible later subsequent precipitation in deeper sediments.

The subsequent overgrowths of calcite at deeper depths were considered to be minor based on the following reasons. At first, two stages of carbonate growth were found but only as a form of aragonite overgrowth on calcite. Authigenic calcites formed earlier than aragonites, and thus calcites are more likely to reflect a pristine PDW composition without secondary alteration. Second, the mean $\delta^{18}O$ and $\delta^{13}C$ values of these calcites at every 1 cm depth interval showed clusters with different core depths (Supplementary Fig. 2). This reflects a time-dependent variability of the fluid composition in a semi-closed system[16], which is strongly supported by the general clustering of the $\delta^{18}O$ and $\delta^{13}C$ values of individual calcite crystals at a limited depth interval (Fig. 3). Marine silicate weathering and subsequent authigenic carbonate precipitation at deeper depths[17] may overprint the authentic PDW record in a semi-closed system. These processes typically release large amounts of Mg (ref. [18].), resulting in dolomite, siderite and Fe-rich calcite formation[17]; however, the Mg contents of authigenic calcite were significantly lower at the deeper depths (Fig. 4). Taken together, we conclude that the geochemical results of authigenic calcites primarily reflect the physicochemical conditions of the overlying PDW without further remarkable diagenetic alteration.

Brackish stadial Arctic. Authigenic calcites at site PS72/410-1 consist of low magnesium calcites (LMC < 4 mol% $MgCO_3$; ref. [19]) during two stadial periods including MIS 4-3 and MIS 2, approximately corresponding to the Middle and Late Weichselian glacial periods[20] (Fig. 4). This observation is in contrast to high magnesium calcites during the Holocene and interstadial within MIS 3 (Fig. 4). The $MgCO_3$ concentrations of calcites are thought to be primarily governed by the Mg/Ca ratios of fluids[21,22]. Over geological time scales, LMC has mainly formed in shallow marine environments during the time intervals of low seawater Mg/Ca (<2 mole/mole), while high magnesium calcites and aragonites have predominantly precipitated during the time intervals of high seawater Mg/Ca (>2) such as the modern condition (~5.2)(review in refs. [19,22]). Laboratory experiments show similar results that $MgCO_3$ concentrations in calcites vary as a function of the aqueous Mg/Ca ratios[23]. Both geological and experimental evidence indicates that the occurrences of the LMC only during stadial periods reflect the significant reduction in Mg/Ca ratios of the PDW in the western Arctic Ocean. This reduction cannot be achieved by oceanic mixing between the Arctic Ocean and surrounding oceans because Mg/Ca ratios of deep seawater are generally homogenous[24]. An intrusion of cold hydrocarbon seepage that is thought to be responsible for the LMC precipitation in today's aragonite sea[25–27] might be considered. Hydrocarbon seepage in the Arctic is generally associated with the destabilization of gas hydrate, possibly via bottom temperature warming[28,29] and/or isostatic rebound by glacial unloading[30]. Given the depth of the coring site, however, it is difficult to
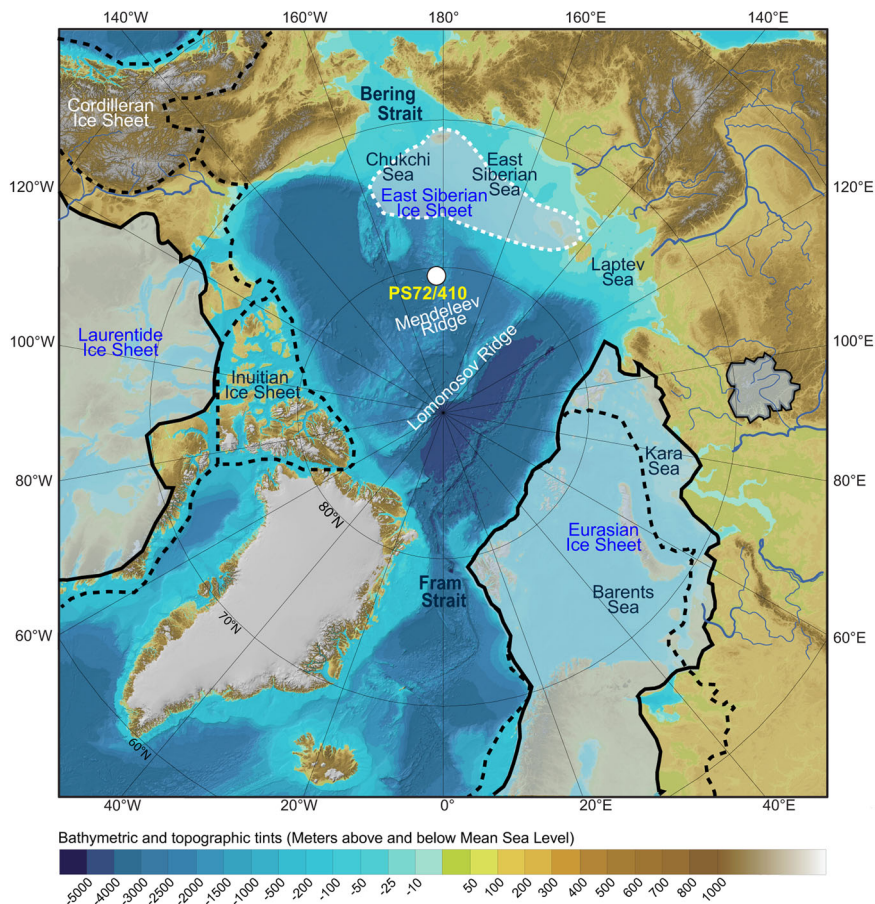
Fig. 1 Location of the study area and sampling locality in the Arctic Ocean. Sediment core PS72/410-1 was collected from the central part of the Mendeleev Ridge in the western Arctic at 80°N at a water depth of 1,800 m during RV *Polarstern* Arctic Expedition ARK-XXIII/3 (PS72) in 2008 using a giant box corer[15]. The maximum extents of the Laurentide Ice Sheet and Eurasian Ice Sheet during the last glacial maximum (black dotted lines) and MIS 4 (solid black lines) are marked[93]. A white dotted line indicates the Quaternary maximum extent of the marine-based East Siberian Ice Sheet[80]. The bathymetry is taken from IBCAO Ver. 3.0 (ref. [94]).

envisage a mechanism to destabilize gas hydrates during glacial periods. In addition, our data with positive $\delta^{13}C$ signatures (Fig. 4) are in contrast to typical negative data derived from the oxidation of methane hydrates[31].

Freshwater typically shows an order of magnitude lower Mg/Ca ratios compared to seawater, which is also consistent with the case in the Arctic Ocean[32–34] (Supplementary Table 1). Therefore, the massive sinking of freshwater could account for the significant reduction in the seawater Mg/Ca ratio, thereby precipitating the LMC during two stadial periods. This is also strongly supported by generally lower strontium (Sr) contents in the LMC (Supplementary Fig. 3), typically resulting from carbonate precipitation in low Sr/Ca ratios of fluid[35], which is attributable to low salinity condition as evident from lower Sr/Ca ratios of freshwater[32,33] than seawater[24] in the Arctic Ocean. During glacial periods, freshwater discharge in the Arctic was prevalent due to the waxing and waning of continental ice sheets[20], and its intrusion into the PDW occurred as recorded by conventional water mass tracer, authigenic ε_{Nd} (ref. [15]) (Fig. 4). The time-dependent variability of calcite $\delta^{18}O$ additionally supports the freshwater sinking idea, as inferred from the general correlation between the MgCO$_3$ contents and $\delta^{18}O$ values of authigenic calcite ($r \sim 0.6$, $n = 22$) (Supplementary Fig. 4). The changes in $\delta^{18}O$ typically result from changes in ambient seawater temperature, but a wide $\delta^{18}O$ range of ~11‰ of the authigenic calcites does not correspond to temperature variability during the last glacial-interglacial cycle[36] because the temperature

estimation range based on the ^{18}O range is far larger than the present PDW temperature range ($-0.7 \sim -0.9$ °C at ~2000 m depth from ref. [9]). The calcite $\delta^{18}O$ signatures instead likely record the compositional change in the PDW in response to freshwater intrusion (Fig. 4). Terrestrial freshwater such as Arctic rivers release highly depleted $\delta^{18}O$ (-23.8 to -16.3 ‰ VSMOW; refs. [37,38]), resulting in negative $\delta^{18}O$ values near the river mouths on the Kara, Laptev and Beaufort shelves at present[37]. Following this observation, light $\delta^{18}O$ signatures of planktic foraminifers in multiple sediment cores from the Arctic Ocean since the penultimate glacial including MIS 4-3 and 2 (e.g., refs. [15,39]) could be primarily attributed to $\delta^{18}O$-depleted freshwater discharge, and the associated lower $\delta^{18}O$ values of the LMC in this study could reflect its sinking into the PDW. For example, general lower calcite $\delta^{18}O$ values associated with higher authigenic ε_{Nd} during MIS 4-3 can be interpreted as the intrusion of $\delta^{18}O$-depleted freshwater[37,38], likely originating from the Eurasian Ice Sheet[20,40] and perhaps also the East Siberian Ice Sheet[39] (Fig. 4). Likewise, negative $\delta^{18}O$ values during MIS 2 could be explained by freshwater sinking, possibly derived from the Laurentide Ice Sheet on N. America as recorded in lower authigenic ε_{Nd}[15] (Fig. 4).

The PDW-freshening scenario is broadly consistent with the recent suggestion based on the excess thorium-230 ($^{230}Th_{ex}$) in the marine sediments from the Arctic Ocean and the Nordic Seas[5], but there are two important discrepancies between the studies. First, we determine that the PDW was brackish rather
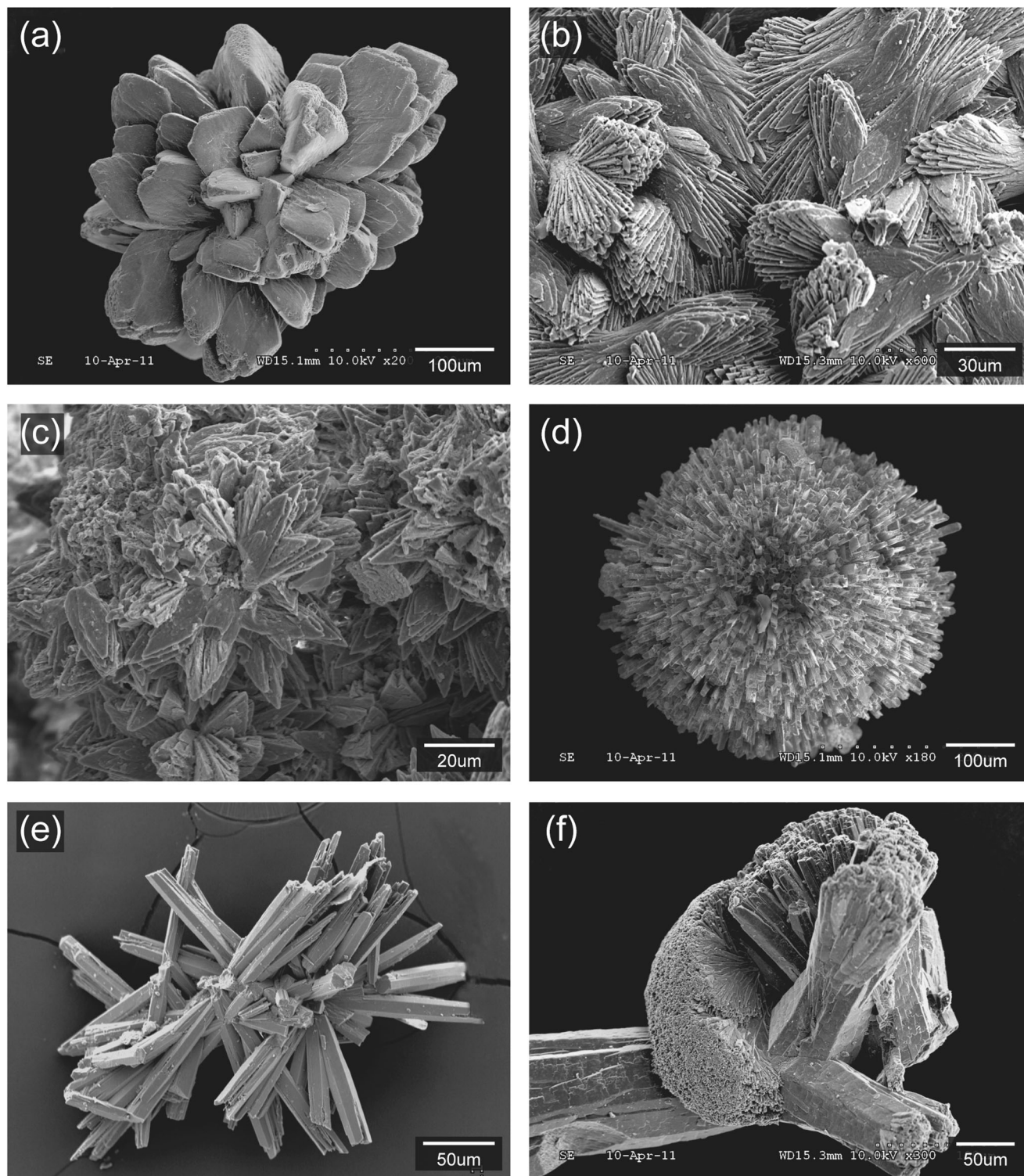
Fig. 2 Scanning electron microscopy (SEM) photomicrographs showing a variety of calcite and aragonite ultrastructures of authigenic carbonates.
a Radially grown calcite lumps with foliated layers, **b** randomly oriented, foliated calcite, **c** radially oriented, foliated calcite, **d** spherulitic aragonite, **e** randomly oriented aragonite crystals with square-ended terminations, and **f** two stages of aragonite growth. Note that larger aragonite rods are overgrown by finer spherulitic fibrous aragonite.

than fresh. Geibert et al.[5] showed a widespread disappearance of $^{230}Th_{ex}$ in Arctic and subarctic deep-sea sediments during portions of MIS 6 and 4, from which they suggested that these regions were fully filled by freshwater. In this extreme condition, the presence of microfossils may result from sediment reworking as proposed by the original author[5,6], but continuous $\delta^{18}O$ records of foraminifers in the Nordic Seas and the Fram Strait are consistent with other global deep-sea records, casting doubt on this hypothesis (for details, see ref. [7]). On the other hand, our simple mass balance calculation based on calcite $\delta^{18}O$ at site PS72/410-1 tentatively suggests that the seawater in the western Arctic Ocean above the depth of 1,800 m would have been diluted
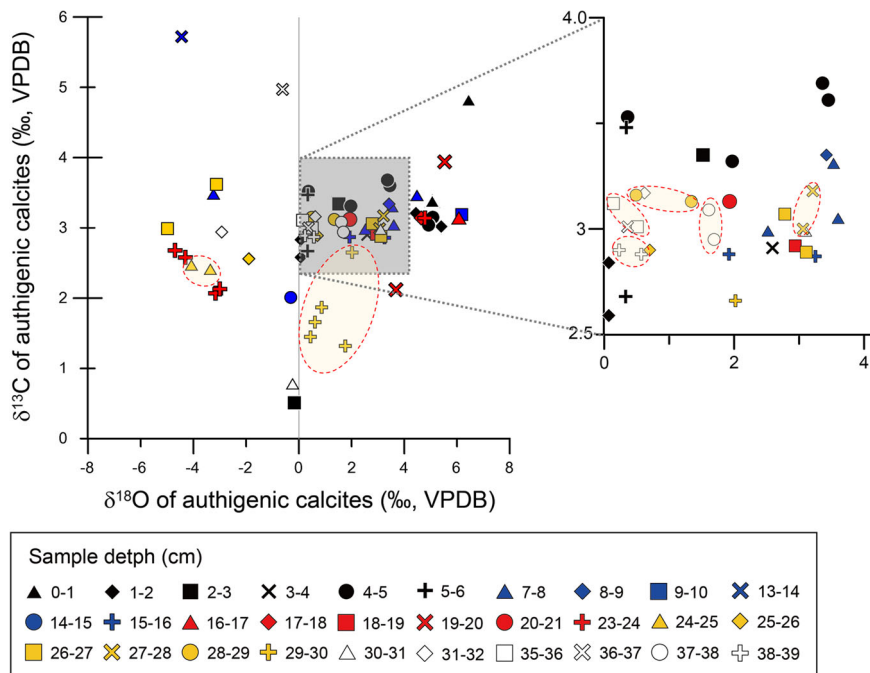
Fig. 3 Scatter diagram of carbon versus oxygen isotope compositions for authigenic calcites with sampling depth. At every 1 cm depth interval, carbon and oxygen isotope compositions tend to cluster to some extent, showing a semi-closed diagenetic system[16]. This clustering implies that the stable isotope contents of authigenic calcites may adequately reflect the PDW conditions when they precipitated.
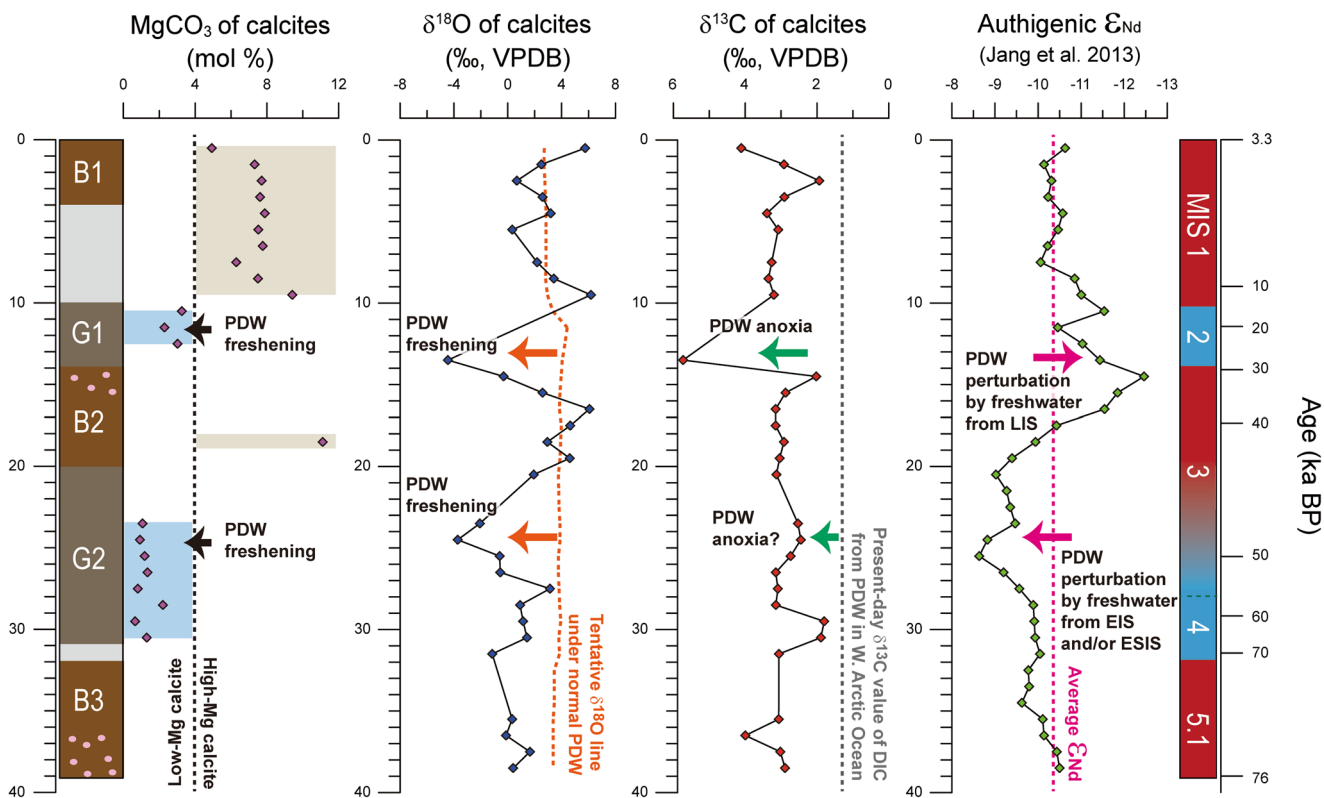

Fig. 4 Downcore variability in MgCO₃ concentrations and stable isotope values ($\delta^{18}O$ and $\delta^{13}C$) of authigenic calcites as well as authigenic ε_{Nd} at site PS72/410-1. Geochemical records indicate brackish and anoxic environments of the deep Arctic Ocean during stadial periods, resulting from oxygen-depleted freshwater intrusion, as recorded by authigenic ε_{Nd}. Note that data is absent at 13–18, 19–23 and 31–39 cm for Mg contents and 10–13, 21–23 and 32–35 cm for stable isotopes.
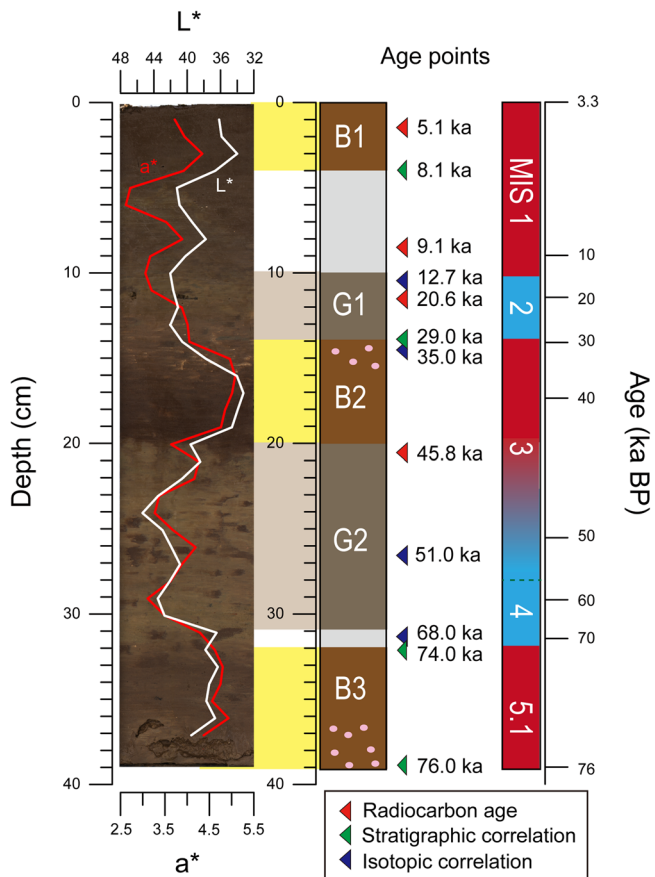
Fig. 5 Revised lithostratigraphy and age models. Depth intervals for lithostratigrapphic Units G1, B2, and G2 were adjusted primarily based on colour reflectance L* values and radiocarbon ages. The age model was applied based on the previous construction using radiocarbon ages and by correlating lithostratigraphy and stable isotopes of planktic foraminifers with neighbouring cores[15]. The age for core-top sediments was estimated by linear extrapolation.

by freshwater by up to 40% (Supplementary Note 4). This covers the brackish (>21‰) to saline water conditions rather than freshwater. These brackish conditions are commensurate with the presence of foraminifera, given the tolerance of foraminifera to lower salinity[41,42] (for details, see the next section). Second, there is a slight discrepancy in the timing for the PDW freshening events between our (MIS 4 to early MIS 3) and previous studies (MIS 4). However, both LMC and $^{230}Th_{ex}$ minima occurred within the same lithostratigraphic Unit G2, and thus the time discrepancy would be interpreted as an artefact of age uncertainty induced by applying different age models. In contrast to our study, Geibert et al.[5] did not adopt the widely accepted age model in the central Arctic Ocean based on radiocarbon ages and nannofossil occurrences (e.g., ref. [43]) but instead assigned low $^{230}Th_{ex}$ intervals to MIS 6 and 4 through correlation to the corresponding $^{230}Th_{ex}$ minima at site PS1533-3 from the Yermak Plateau. Indeed, the disappearance of $^{230}Th_{ex}$ was found at the upper part of Unit G2 of the nearby core PS72/396-3 (80°34.74'N, 162°19.01'W, 2722 m water depth; ref. [5]), which was dated to 45.8 ka BP in our core (Fig. 5). Furthermore, we also suggest MIS 2 as an additional freshening interval, which was partly identified by the $^{230}Th_{ex}$ minima in the selected cores[5]. The less pronounced $^{230}Th_{ex}$ record is probably attributed to the poor preservation of sedimentary records during the last glacial maximum[15,44–46], which may have resulted in the diluted $^{230}Th_{ex}$ inventories[5]. The

reduced $^{230}Th_{ex}$ records for Arctic sediments[47,48] during MIS 2 may support this speculation.

Anoxic PDW during cold stadials. Despite the massive freshwater intrusion into the PDW, the PDW was probably oxygendepleted during MIS 2. During this period, the $\delta^{13}C$ value of authigenic calcite at site PS72/410-1 reaches a maximum of 5.7 ‰. Considering a slight enrichment by ca. 1 per mil between calcite and bicarbonate in seawater[49], this positive $\delta^{13}C$ value is much higher than those of dissolved inorganic carbon (DIC; 1.26 ± 0.12‰ from ref. [50]) and live benthic foraminifera *C. wuellerstorfi* in the deep Amerasian Basin of the western Arctic Ocean (1.44 ± 0.10‰ from ref. [50]) (Fig. 4). Similar to calcite $\delta^{18}O$ values, massive freshwater sinking may exert an influence on the calcite $\delta^{13}C$ values, however, the observed change in $\delta^{13}C$ is not consistent with the negative $\delta^{13}C$ signatures of the Arctic rivers at present (-8‰ on average from refs. [51,52]). While the negative $\delta^{13}C$ excursion is expected from PDW freshening, the actual increase in $\delta^{13}C$ can be caused by one of the following factors: (i) oxidation of marine organic matter, (ii) methane oxidation, (iii) dissolution of carbonates in sediments and (iv) microbial methanogenesis. However, the first and second factors can be simply discarded because both typically result in negative shifts in the $\delta^{13}C$ of authigenic carbonates down to −25 and −75‰, respectively[53,54]. Carbonate dissolution is also not likely since carbonate rocks from the Mackenzie River drainage, which is the primary source area for Arctic carbonates, have relatively low $\delta^{13}C$ signatures ranging from −3.6 to +2.8‰ (after converting into VPDB scale from ref. [51]). On the other hand, methanogenesis can cause ^{13}C enrichment and even positive $\delta^{13}C$ (ref. [17,54]), thus accounting for the positive $\delta^{13}C$ signatures of the authigenic calcites at site PS72/410-1. Methanogenesis is an anaerobically organic respiration process that generates methane (CH_4). In these reactions, CH_4 preferentially uptakes light carbon (^{12}C). The production of ^{13}C-depleted CH_4 under the semi-closed system renders residual dissolved inorganic carbon pools to be enriched in ^{13}C, thereby forming the ^{13}C-enriched authigenic calcites at the sediment-water interface under anoxic conditions.

The conventional explanations for ocean anoxia include decreased vertical mixing that limits oxygen supply (e.g., ref. [3]) or the increased respiration of labile organic matter that consumes oxygen (e.g., ref. [55]). However, the idea of reduced vertical mixing can be excluded based on our earlier statement that the vigorous sinking of freshwater took place. In addition, in the central Arctic sediment cores during glacial periods, organic carbon accumulation is known to be generally lower[56] than in present-day oxygenated conditions[8]. Indeed, the contents of total organic carbon at site PS72/410-1 are relatively higher during the Holocene compared to the last glacial period, even after correcting time-dependent decrease in total organic carbon by organic matter degradation[57,58] (Supplementary Fig. 1). Thus, we conclude that in-situ oxygen consumption by organic matter respiration does not solely induce the anoxic PDW during MIS 2, calling for an additional process.

It can be speculated that the meltwater which filled the PDW was oxygen-poor freshwater, which can be generally noticed at the base of glaciers[59,60]. During cold stadial periods such as MIS 2 (refs. [20,61]), massive ice sheets had expanded on the shelves and adjacent land areas in the Arctic Ocean. This led to vigorous glacial erosion, potentially resulting in substantial storage of sediments with the terrigenous organic matter within ice sheets[57,62,63]. The influence of this organic matter seemed to be not distinct beyond the shelf edge[64] as indicated by the absence of a decrease in $\delta^{13}C_{org}$ at site PS72/410-1 during MIS 2 (Supplementary Note 5 and Supplementary Fig. 1). However,
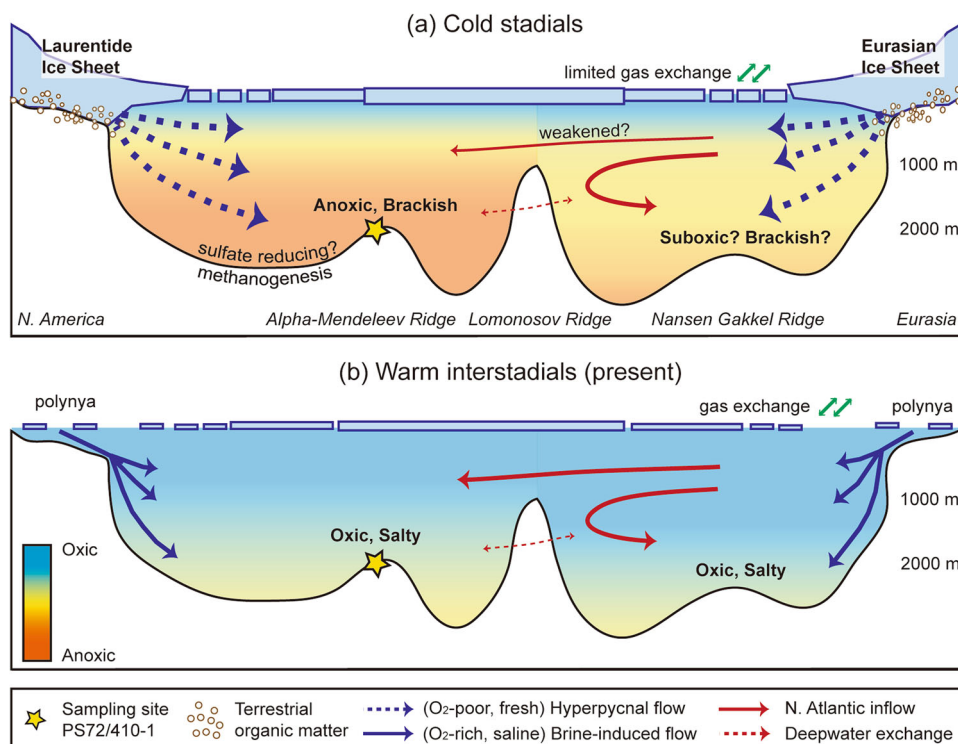
Fig. 6 Schematic illustrations of the oceanic conditions in the Arctic Ocean during two contrasting periods. The anoxic subglacial meltwater underneath the Laurentide and Eurasian Ice Sheets (potentially also East Siberian Ice Sheet; not shown) formed sediment-laden hyperpycnal flows, leading to PDW freshening and anoxia during stadials (**a**), while brine formation at the marginal polynya can supply oxygen into the deep basin by vertical mixing during interstadials (**b**). We speculate that oxygen contents in the eastern Arctic Ocean during stadials were slightly more oxygenated than those in the western Arctic Ocean due to limited, but continuous exchange with the North Atlantic inflow. Note that the deep water exchange below ~1700 m was likely limited based on the present-day observation that deep water in the western Arctic Ocean crosses the Lomonosov Ridge through the passages in the intra-basin near the North Pole (~1870 m)[75,76] or the southern passage of the southern Lomonosov Ridge (~1700 m)[77], but the water inflow in the opposite way has been yet observed at the depth shallower than ~1700 m[77].

higher TOC contents on the Chukchi Borderland[62] and the Siberian continental margin[65] during early MIS 2 suggest the enhanced input of terrestrial organic matter within the boundaries of the shelf, which potentially exerted a strong influence on the regional water chemistry[66]. Indeed, subglacial environments under ice sheets are known to be largely anoxic[67] due to restricted atmospheric exchange and enhanced microbial organic respiration[60,68]. Hence, it is likely that the meltwater discharged beneath ice sheets during MIS 2 was essentially oxygen-poor, which was possibly sustained by the prolonged meltwater residence time[69] as well as the limited air-sea exchange under thick perennial sea ice or an ice shelf as inferred from geomorphological features on the continental shelf and submarine ridges in the western Arctic Ocean (refs. [70,71]).

The subglacial meltwater from ice sheets contained large amounts of sediments, episodically forming high-density flows[72] that resulted in vigorous deep intrusion[47] at all depth levels depending upon the density (Fig. 6). During its journey into the deep sea, the density of hyperpycnal flows may have decreased by sediment settling, however, the flows could have maintained their physical characteristics over long distances through the entrainment of ambient seawater[73]. While the oxygen-depleted subglacial water could thus reach and influence seawater at all depth levels, the PDW would have become further deoxygenated in conjunction with in-situ organic decomposition. As the process progressed, a very thin sulfate-reducing zone seemed to disappear near the sediment-seawater interface due to the strong anoxic condition of overlying seawater, and then the sediment near the seafloor directly transitioned into the methanogenic zone. In

combination with massive meltwater discharge[39], the inferred existence of thick perennial sea ice or an ice shelf covering the Arctic Ocean during cold stadials including MIS 4 and 2 (refs. [5,70,71,74]) may have notably inhibited Atlantic water inflow carrying salt and oxygen (Fig. 6), possibly allowing a semi-enclosed western Arctic basin to maintain brackish and anoxic PDW.

The presence of calcareous foraminifers under brackish and anoxic conditions is, at first, difficult to explain[6]. Indeed, many Arctic sediment cores showed barren to low foraminifers in lithostratigraphic Unit G1, typically corresponding to MIS 2 (e.g., ref. [11]). However, given the extremely low sedimentation rate during this interval (~0.2 cm kyr^{-1} at core PS72/410-1), the discontinuity of these unfavourable conditions for the growth of foraminifers in conjunction with a tolerance of foraminifers[41,42] may provide a key clue to explain a few (rare) occurrences of foraminifers during MIS 2. The entrained seawater into hyperpycnal flows likely supplied intermittent extra oxygen and salt into the deep sea, allowing the presence of benthic fauna for short time intervals until the oxygen was exhausted. The relatively oxygenated and saline N. Atlantic inflow from the eastern Arctic to the western Arctic might also be a potential feeder although their inflow would be the minimum, given the presence of a thick ice shelf at least above ~450 m on the continental shelf in the western Arctic Ocean during MIS 2 (refs. [70,71]), and a lack of observation for deepwater inflow from the eastern Arctic Ocean below ~1700 m (refs. [75–77]). Episodic ecosystem recovery under prevalent anoxic environments is exemplified by the re-establishment of benthic fauna during sapropel formation in

the Mediterranean (e.g., ref. [78]) where the sedimentation rate is much higher (6.8–13.7 cm kyr[-1] from ref. [79]). In this view, the general absence of foraminifera between 13-19 ka BP in sediment cores from the Mendeleev Ridge[11] might be interpreted as a prolonged of anoxia and freshening.

Interestingly, the δ^{13}C signatures during the other intervals are also positive although the magnitudes are not highly pronounced (Fig. 4). These positive δ^{13}C excursions were perhaps attributable to persistent anoxic environments like during MIS 2. This could also be likely during MIS 4-3 because calcareous microfossils also rarely occurred[5,11], and meltwater intrusion with negative δ^{13}C (refs. [51,52]) may have suppressed the positive δ^{13}C signatures from methanogenesis. However, brown layers, corresponding to the Holocene and interstadial within MIS 3 (ref. [80]), contain relatively abundant benthic foraminifers in the western Arctic Ocean (e.g., ref. [11]). A combination of reduced meltwater supply, the increased role of water temperature in the density structure of the ocean, and the strong formation of brine via seasonal sea ice formation on the continental margin[81] may have contributed to deep convection, thereby supplying oxygen and salt to the PDW for these benthic fauna (Fig. 6). Therefore, slight increases in δ^{13}C during warm periods may not reflect methanogenesis but rather a natural variability of seawater δ^{13}C in response to changes in surface productivity, air-sea exchange rate and water circulation[82]. Our anoxic scenario is not fully supported by authigenic uranium enrichment, another traditional indicator for reducing environments, in Arctic sediment cores during stadials[5]. This inconsistency is probably not due to the non-reducing setting but due to the very limited concentration of dissolved uranium in seawater by freshening, as inferred from a widespread disappearance of [230]Th$_{ex}$ at those times[5].

Overall, we conclude that the PDW in the western Arctic Ocean was predominantly brackish and oxygen-depleted during stadial periods such as MIS 4-3 and MIS 2. Significantly reduced oxygen concentrations during glacial periods have also been reported in the Southern Ocean[3] and the North[83] and South Atlantic[84], implying ubiquitous oxygen depletion events in the glacial deep ocean realm. Considering the general relationship between the dissolved oxygen concentrations and the amounts of respired carbon in the oceanic water mass[83], a substantial amount of carbon could be stored in the PDW of the western Arctic Ocean, serving as an important carbon sink during glacial periods. The hyperpycnal subglacial meltwater probably acted as the primary carrier of the glacially derived carbon (organic carbon, CO_2 and CH_4) from beneath continental ice sheets to the deep ocean before escaping into the atmosphere. Future work for quantitative O_2 reconstructions across the entire Arctic Ocean will provide a more complete perspective on the behaviour of greenhouse gases across glacial-interglacial cycles.

Methods

Core information. Sediment core PS72/410-1 was collected using a giant box corer in the central part of the Mendeleev Ridge in the western Arctic during RV *Polarstern* Expedition ARK-XXIII/3 (PS72) in 2008 (80.51°N, 175.74°W; water depth of 1800 m) (Fig. 1). Core PS72/410-1 is mainly composed of sandy-silty clay with varying colours of brown to dark brown, dark yellowish brown, olive to olive-brown, and dark greyish brown[15,85]. In this study, we propose the revised lithostratigraphy based on the reported radiocarbon ages and colour reflectance L* values[15] for better consistency between cores in the western Arctic Ocean (Fig. 5). In brief, the brownish Units B1 and B3 were defined as the depth intervals of 0–4 cm and 32–39 cm, in agreement with the previous study[15]. On the other hand, the depth interval of lithostratigraphic Unit G1 was modified to be 10–14 cm based on the radiocarbon ages as well as high L* values to match its updated age assignment to the last glaciation/deglaciation[80,86]. Likewise, the depth intervals for underlying Units B2 and G2 were slightly adjusted to 14–20 cm with low L* and 20–31 cm with high L*, respectively. We generally adopted the previous age model based on radiocarbon age dating and isotopic and stratigraphic correlations with neighbouring cores[15]. However, given the uncertainty of carbon reservoir time in the Arctic Ocean (ΔR = 1000 yr applied in this study from ref. [87]), the bottom of

Unit G1 was assigned to the end of MIS 2 for better consistency with the Arctic cores[80,86] (Fig. 5) although radiocarbon age was dated to 30.8 ka BP at corresponding depth[15]. In addition, we used the extrapolated age of the surface sediments (0–1 cm) rather than zero because of the low sedimentation rate during the late Holocene due to the presence of perennial sea ice (e.g., ref. [88]). Thus, the age of core PS72/410-1 spans 76 to 3.3 ka BP.

Authigenic carbonate analysis. A 39-cm-thick sediment core was subsampled at 1-cm intervals for textural and geochemical analyses. After wet sieving (63 μm), carbonate crystals were hand-picked under a binocular microscope. Carbonate crystals were examined with binocular and scanning electron microscopes for textural analysis. Carbonate mineralogy was determined by crystal shapes (square-ended terminations of aragonite crystals) and qualitative EDAX analysis (high Sr and low Mg contents for aragonite and low Sr and high Mg contents for calcite). Carbonate crystals were separated by repetitive density separation using a chemical agent produced in the laboratory[89]. The chemical reagent caused the fluids (the mixture of sodium polytungstate and distilled water) to have a density of 2.8 g cm^{-3}, thereby separating calcite from aragonite. The crystal shape and microstructure were examined using a scanning electron microscope (S-4300, Hitachi) at the Korea Institute of Ocean Science and Technology. The relative proportions of authigenic carbonates in the sediments were qualitatively determined to be low, middle, and high.

Stable isotope analysis on carbonate crystals was carried out using a Finnigan MAT253 gas mass spectrometer with a Kiel IV automatic carbonate preparation device at the Alfred Wegener Institute. The mass spectrometer was calibrated via the international standard NBS19 to the VPDB scale, and the results are given in δ-notation versus VPDB. The precisions of the δ^{18}O and δ^{13}C values, based on the periodic measurements of an internal laboratory standard (Solnhofen limestone) over one year, were better than 0.08 and 0.06‰, respectively[50]. Magnesium concentrations of authigenic carbonates were analysed using inductively coupled plasma atomic emission spectroscopy (Ultima 2 C, Horiba Jobin Yvon) at the Korea Basic Science Institute with a relative standard deviation of <5%. All data generated in this study can be found in a public repository in the Korea Polar Data Center[90].

References

1. Ahn, J. & Brook, E. J. Atmospheric CO_2 and climate on millennial time scales during the last glacial period. *Science* **322**, 83–85 (2008).
2. Sigman, D. M. et al. The Southern Ocean during the ice ages: a review of the Antarctic surface isolation hypothesis, with comparison to the North Pacific. *Quat. Sci. Rev.* **254**, 106732 (2021).
3. Lu, Z. et al. Oxygen depletion recorded in upper waters of the glacial Southern Ocean. *Nat. Commun.* **7**, 1–9 (2016).
4. Jakobsson, M. et al. Manganese and color cycles in Arctic Ocean sediments constrain Pleistocene chronology. *Geology* **28**, 23–26 (2000).
5. Geibert, W., Matthiessen, J., Stimac, I., Wollenburg, J. & Stein, R. Glacial episodes of a freshwater Arctic Ocean covered by a thick ice shelf. *Nature* **590**, 97–102 (2021).
6. Geibert, W., Matthiessen, J., Wollenburg, J. & Stein, R. Reply to: No freshwater-filled glacial Arctic Ocean. *Nature* **602**, E4–E6 (2022).
7. Spielhagen, R. F., Scholten, J. C., Bauch, H. A. & Eisenhauer, A. No freshwater-filled glacial Arctic Ocean. *Nature* **602**, E1–E3 (2022).
8. Woodgate, R. A., Aagaard, K., Swift, J. H., Smethie Jr, W. M. & Falkner, K. K. in *Chukchi Borderland Cruise CBL2002 Arctic West - Phase II (AWS-02-II)*. 51 (University of Washington, Seattle, WA, USA, 2002).
9. Jones, E., Rudels, B. & Anderson, L. Deep waters of the Arctic Ocean: origins and circulation. *Deep-Sea Res. I* **42**, 737–760 (1995).
10. Farmer, J. R. et al. Arctic Ocean stratification set by sea level and freshwater inputs since the last ice age. *Nat. Geosci.* **14**, 684–689 (2021).
11. Polyak, L., Curry, W. B., Darby, D. A., Bischof, J. & Cronin, T. M. Contrasting glacial/interglacial regimes in the western Arctic Ocean as exemplified by a sedimentary record from the Mendeleev Ridge. *Palaeogeogr. Palaeoclimatol. Palaeoecol.* **203**, 73–93 (2004).

12. Ezat, M. M., Rasmussen, T. L., Skinner, L. C. & Zamelczyk, K. Deep ocean ^{14}C ventilation age reconstructions from the Arctic Mediterranean reassessed. *Earth Planet. Sci. Lett.* **518**, 67–75 (2019).

13. Folk, R. L. The natural history of crystalline calcium carbonate; effect of magnesium content and salinity. *J. Sediment. Res.* **44**, 40–53 (1974).

14. Jutterström, S. & Anderson, L. G. The saturation of calcite and aragonite in the Arctic Ocean. *Mar. Chem.* **94**, 101–110 (2005).

15. Jang, K. et al. Glacial freshwater discharge events recorded by authigenic neodymium isotopes in sediments from the Mendeleev Ridge, western Arctic Ocean. *Earth Planet. Sci. Lett.* **369-370**, 148–157 (2013).

16. Woo, K. S. & Khim, B.-K. Stable oxygen and carbon isotopes of carbonate concretions of the Miocene Yeonil Group in the Pohang Basin, Korea: types of concretions and formation condition. *Sediment. Geol.* **183**, 15–30 (2006).

17. Torres, M. E. et al. Silicate weathering in anoxic marine sediment as a requirement for authigenic carbonate burial. *Earth-Sci. Rev.* **200**, 102960 (2020).

18. Wallmann, K. et al. Silicate weathering in anoxic marine sediments. *Geochim. Cosmochim. Acta* **72**, 2895–2918 (2008).

19. Stanley, S. M. Effects of global seawater chemistry on biomineralization: past, present, and future. *Chem. Rev.* **108**, 4483–4498 (2008).

20. Svendsen, J. I. et al. Late Quaternary ice sheet history of northern Eurasia. *Quat. Sci. Rev.* **23**, 1229–1271 (2004).

21. Hardie, L. A. Secular variation in seawater chemistry: an explanation for the coupled secular variation in the mineralogies of marine limestones and potash evaporites over the past 600 m.y. *Geology* **24**, 279–283 (1996).

22. Ries, J. B. Geological and experimental evidence for secular variation in seawater Mg/Ca (calcite-aragonite seas) and its effects on marine biological calcification. *Biogeosciences* **7**, 2795–2849 (2010).

23. De Choudens-Sánchez, V. & González, L. A. Calcite and aragonite precipitation under controlled instantaneous supersaturation: elucidating the role of CaCO3 saturation state and Mg/Ca ratio on Calcium Carbonate polymorphism. *J. Sediment. Res.* **79**, 363–376 (2009).

24. Lebrato, M. et al. Global variability in seawater Mg:Ca and Sr:Ca ratios in the modern ocean. *Proc. Natl. Acad. Sci. USA* **117**, 22281–22292 (2020).

25. Feng, D., Roberts, H. H., Joye, S. B. & Heydari, E. Formation of low-magnesium calcite at cold seeps in an aragonite sea. *Terra Nova* **26**, 150–156 (2014).

26. Nehza, O. et al. The origin of cold-water authigenic carbonates from deep-water, muddy sediments in the Ulleung Basin, East Sea of Korea. *Geosci. J.* **16**, 25–34 (2012).

27. Huang, H. et al. New constraints on the formation of hydrocarbon-derived low magnesium calcite at brine seeps in the Gulf of Mexico. *Sediment. Geol.* **398**, 105572 (2020).

28. Mienert, J. et al. Ocean warming and gas hydrate stability on the mid-Norwegian margin at the Storegga Slide. *Mar. Petrol. Geol.* **22**, 233–244 (2005).

29. Ferré, B. et al. Reduced methane seepage from Arctic sediments during cold bottom-water conditions. *Nat. Geosci.* **13**, 144–148 (2020).

30. Wallmann, K. et al. Gas hydrate dissociation off Svalbard induced by isostatic rebound rather than global warming. *Nat. Commun.* **9**, 1–9 (2018).

31. Yao, H., Niemann, H. & Panieri, G. Multi-proxy approach to unravel methane emission history of an Arctic cold seep. *Quat. Sci. Rev.* **244**, 106490 (2020).

32. Reeder, S. W., Hitchon, B. & Levinson, A. A. Hydrogeochemistry of the surface waters of the Mackenzie River drainage basin, Canada—I. Factors controlling inorganic composition. *Geochim. Cosmochim. Acta* **36**, 825–865 (1972).

33. Huh, Y., Tsoi, M.-Y., Zaitsev, A. & Edmond, J. M. The fluvial geochemistry of the rivers of Eastern Siberia: I. tributaries of the Lena River draining the sedimentary platform of the Siberian Craton. *Geochim. Cosmochim. Acta* **62**, 1657–1676 (1998).

34. Vorobyev, S. N. et al. Biogeochemistry of dissolved carbon, major, and trace elements during spring flood periods on the Ob River. *Hydrol. Process.* **33**, 1579–1594 (2019).

35. Ingram, B. L., De Deckker, P., Chivas, A. R., Conrad, M. E. & Byrne, A. R. Stable isotopes, Sr/Ca, and Mg/Ca in biogenic carbonates from Petaluma Marsh, northern California, USA. *Geochim. Cosmochim. Acta* **62**, 3229–3237 (1998).

36. Hillaire-Marcel, C. & Ravelo, A. The use of Oxygen and Carbon isotopes of foraminifera in paleoceanography. *Dev. Mar. Geol.* **1**, 735–764 (2007).

37. Bauch, D., Erlenkeuser, H. & Andersen, N. Water mass processes on Arctic shelves as revealed from δ^{18}O of H2O. *Glob. Planet. Chang.* **48**, 165–174 (2005).

38. Cooper, L. W. et al. Linkages among runoff, dissolved organic carbon, and the stable oxygen isotope composition of seawater and other water mass indicators in the Arctic Ocean. *J. Geophys. Res. Biogeo.* https://doi.org/10.1029/2005JG000031 (2005).

39. Zhao, S. et al. Sedimentary record of glacial impacts and melt water discharge off the East Siberian Continental Margin, Arctic Ocean. *J. Geophys. Res. Oceans* **127**, e2021JC017650 (2022).

40. Mangerud, J. et al. Ice-dammed lakes and rerouting of the drainage of northern Eurasia during the Last Glaciation. *Quat. Sci. Rev.* **23**, 1313–1332 (2004).

41. Greco, M., Meilland, J., Zamelczyk, K., Rasmussen, T. L. & Kucera, M. The effect of an experimental decrease in salinity on the viability of the Subarctic planktonic foraminifera Neogloboquadrina incompta. *Polar Res.* **39**, 1–8 (2020).

42. Saraswat, R. et al. Effect of salinity induced pH/alkalinity changes on benthic foraminifera: a laboratory culture experiment. *Estuar. Coast. Shelf S.* **153**, 96–107 (2015).

43. Spielhagen, R. F. et al. Arctic ocean deep-sea record of northern Eurasian ice sheet history. *Quat. Sci. Rev.* **23**, 1455–1483 (2004).

44. Nørgaard-Pedersen, N., Spielhagen, R. F., Thiede, J. & Kassens, H. Central Arctic surface ocean environment during the past 80,000 years. *Paleoceanography* **13**, 193–204 (1998).

45. Poore, R. Z., Osterman, L., Curry, W. B. & Phillips, R. L. Late Pleistocene and Holocene meltwater events in the western Arctic Ocean. *Geology* **27**, 759–762 (1999).

46. Polyak, L. et al. Late Quaternary stratigraphy and sedimentation patterns in the western Arctic Ocean. *Glob. Planet. Chang.* **68**, 5–17 (2009).

47. Hoffmann, S. S., McManus, J. F., Curry, W. B. & Brown-Leger, L. S. Persistent export of [231]Pa from the deep central Arctic Ocean over the past 35,000 years. *Nature* **497**, 603–606 (2013).

48. Hoffmann, S. & McManus, J. Is there a [230]Th deficit in Arctic sediments? *Earth Planet. Sci. Lett.* **258**, 516–527 (2007).

49. Romanek, C. S., Grossman, E. L. & Morse, J. W. Carbon isotopic fractionation in synthetic aragonite and calcite: Effects of temperature and precipitation rate. *Geochim. Cosmochim. Acta* **56**, 419–430 (1992).

50. Mackensen, A. High epibenthic foraminiferal δ^{13}C in the recent deep Arctic Ocean: implications for ventilation and brine release during stadials. *Paleoceanography* **28**, 574–584 (2013).

51. Hitchon, B. & Krouse, H. R. Hydrogeochemistry of the surface waters of the Mackenzie River drainage basin, Canada—III. Stable isotopes of oxygen, carbon and sulphur. *Geochim. Cosmochim. Acta* **36**, 1337–1357 (1972).

52. Bauch, D., Polyak, L. & Ortiz, J. D. A baseline for the vertical distribution of the stable carbon isotopes of dissolved inorganic carbon (δ[13]C_DIC) in the Arctic Ocean. *Arktos* **1**, 15 (2015).

53. Chow, N., Morad, S. & Al-Aasm, I. S. Origin of authigenic Mn–Fe carbonates and pore-water evolution in marine sediments: evidence from Cenozoic Strata of the Arctic Ocean and Norwegian-Greenland Sea (ODP Leg 151). *J. Sediment. Res.* **70**, 682–699 (2000).

54. Loyd, S. J. & Smirnoff, M. N. Progressive formation of authigenic carbonate with depth in siliciclastic marine sediments including substantial formation in sediments experiencing methanogenesis. *Chem. Geol.* **594**, 120775 (2022).

55. Wehrmann, L. M., Arndt, S., März, C., Ferdelman, T. G. & Brunner, B. The evolution of early diagenetic signals in Bering Sea subseafloor sediments in response to varying organic carbon deposition over the last 4.3Ma. *Geochim. Cosmochim. Acta* **109**, 175–196 (2013).

56. Stein, R. & Macdonald, R. W. in *The Organic Carbon Cycle in the Arctic Ocean* (eds Stein, R. & MacDonald, R. W.) 315–322 (Springer, 2004).

57. Yamamoto, M. & Polyak, L. Changes in terrestrial organic matter input to the Mendeleev Ridge, western Arctic Ocean, during the Late Quaternary. *Glob. Planet. Chang.* **68**, 30–37 (2009).

58. Dong, L. et al. A Eurasian Basin sedimentary record of glacial impact on the central Arctic Ocean during MIS 1–4. *Glob. Planet. Chang.* **219**, 103993 (2022).

59. Mikucki, J. A. et al. A contemporary microbially maintained subglacial ferrous "Ocean". *Science* **324**, 397–400 (2009).

60. Bottrell, S. H. & Tranter, M. Sulphide oxidation under partially anoxic conditions at the bed of the Haut Glacier d'Arolla, Switzerland. *Hydrol. Process.* **16**, 2363–2368 (2002).

61. Batchelor, C. L. et al. The configuration of Northern Hemisphere ice sheets through the Quaternary. *Nat. Commun.* **10**, 1–10 (2019).

62. Rella, S. F. & Uchida, M. Sedimentary organic matter and carbonate variations in the Chukchi Borderland in association with ice sheet and ocean-atmosphere dynamics over the last 155 kyr. *Biogeosciences* **8**, 3545–3553 (2011).

63. Wadham, J. L. et al. Ice sheets matter for the global carbon cycle. *Nat. Commun.* **10**, 3567 (2019).

64. Bröder, L. et al. Fate of terrigenous organic matter across the Laptev Sea from the mouth of the Lena River to the deep sea of the Arctic interior. *Biogeosciences* **13**, 5003–5019 (2016).

65. Martens, J. et al. Remobilization of dormant carbon from Siberian-Arctic permafrost during three past warming events. *Sci. Adv.* **6**, eabb6546 (2020).

66. Semiletov, I. et al. The East Siberian Sea as a transition zone between Pacific-derived waters and Arctic shelf waters. *Geophys. Res. Lett.* https://doi.org/10.1029/2005GL022490 (2005).

67. Stibal, M. et al. Methanogenic potential of Arctic and Antarctic subglacial environments with contrasting organic carbon sources. *Glob. Change Biol.* **18**, 3332–3345 (2012).

68. Wadham, J. L., Bottrell, S., Tranter, M. & Raiswell, R. Stable isotope evidence for microbial sulphate reduction at the bed of a polythermal high Arctic glacier. *Earth Planet. Sci. Lett.* **219**, 341–355 (2004).

69. Wadham, J. L. et al. Biogeochemical weathering under ice: size matters. *Global Biogeochem. Cy.* https://doi.org/10.1029/2009GB003688 (2010).

70. Kim, S. et al. Seismostratigraphic and geomorphic evidence for the glacial history of the northwestern Chukchi margin, Arctic Ocean. *J. Geophys. Res. Earth* **126**, e2020JF006030 (2021).

71. Polyak, L., Darby, D. A., Bischof, J. F. & Jakobsson, M. Stratigraphic constraints on late Pleistocene glacial erosion and deglaciation of the Chukchi margin, Arctic Ocean. *Quat. Res.* **67**, 234–245 (2007).

72. Aharon, P. Entrainment of meltwaters in hyperpycnal flows during deglaciation superfloods in the Gulf of Mexico. *Earth Planet. Sci. Lett.* **241**, 260–270 (2006).

73. Mulder, T., Syvitski, J. P. M., Migeon, S., Faugères, J.-C. & Savoye, B. Marine hyperpycnal flows: initiation, behavior and related deposits. A review. *Mar. Petrol. Geol.* **20**, 861–882 (2003).

74. Ye, L. et al. Late Pleistocene Laurentide-source iceberg outbursts in the western Arctic Ocean. *Quat. Sci. Rev.* **297**, 107836 (2022).

75. Björk, G. et al. Bathymetry and deep-water exchange across the central Lomonosov Ridge at 88–89°N. *Deep-Sea Res. I* **54**, 1197–1208 (2007).

76. Björk, G. et al. Flow of Canadian basin deep water in the Western Eurasian Basin of the Arctic Ocean. *Deep-Sea Res. I* **57**, 577–586 (2010).

77. Björk, G. et al. Bathymetry and oceanic flow structure at two deep passages crossing the Lomonosov Ridge. *Ocean Sci* **14**, 1–13 (2018).

78. Rohling, E. J., Marino, G. & Grant, K. M. Mediterranean climate and oceanography, and the periodic development of anoxic events (sapropels). *Earth-Sci. Rev.* **143**, 62–97 (2015).

79. Casford, J. S. L. et al. A dynamic concept for eastern Mediterranean circulation and oxygenation during sapropel formation. *Palaeogeogr. Palaeoclimatol. Palaeoecol.* **190**, 103–119 (2003).

80. Schreck, M. et al. Improved Pleistocene sediment stratigraphy and paleoenvironmental implications for the western Arctic Ocean off the East Siberian and Chukchi margins. *arktos* **4**, 1–20 (2018).

81. Aagaard, K. & Carmack, E. C. The role of sea ice and other fresh water in the Arctic circulation. *J. Geophys. Res.* **94**, 14485–14498 (1989).

82. Mackensen, A. & Schmiedl, G. Stable carbon isotopes in paleoceanography: atmosphere, oceans, and sediments. *Earth-Sci. Rev.* **197**, 102893 (2019).

83. Hoogakker, B. A., Elderfield, H., Schmiedl, G., McCave, I. N. & Rickaby, R. E. Glacial–interglacial changes in bottom-water oxygen content on the Portuguese margin. *Nat. Geosci.* **8**, 40–43 (2015).

84. Riedinger, N., Scholz, F., Abshire, M. L. & Zabel, M. Persistent deep water anoxia in the eastern South Atlantic during the last ice age. *Proc. Natl. Acad. Sci. USA* **118**, e2107034118 (2021).

85. Jokat, W. in *Berichte zur Polar und Meeresforschung* 1–222 (Alfred Wegener Institute for Polar and Marine Research, 2009).

86. Joe, Y. J. et al. Late Quaternary depositional and glacial history of the Arliss Plateau off the East Siberian margin in the western Arctic Ocean. *Quat. Sci. Rev.* **228**, 106099 (2020).

87. Hanslik, D. et al. Quaternary Arctic Ocean sea ice variations and radiocarbon reservoir age corrections. *Quat. Sci. Rev.* **29**, 3430–3441 (2010).

88. de Vernal, A. et al. Natural variability of the Arctic Ocean sea ice during the present interglacial. *Proc. Natl. Acad. Sci. USA* **117**, 26069–26075 (2020).

89. Douka, K., Hedges, R. E. M. & Higham, T. F. G. Improved AMS ^{14}C dating of shell carbonates using high-precision X-ray diffraction and a novel density separation protocol (cards). *Radiocarbon* **52**, 735–751 (2010).

90. Jang, K., Nam, S.-I., Woo, K. S. & Kim, J.-K. Geochemical dataset measured from authigenic carbonates and bulk sediments in core PS72/410-1. *Korea Polar Data Center.* https://doi.org/10.22663/KOPRI-KPDC-00002173.2 (2023).

91. Jang, K. et al. Neodymium isotope ratios of the authigenic fractions in sediment core PS72/410-1. *PANGAEA.* https://doi.org/10.1594/PANGAEA.817611 (2013).

92. Jang, K. et al. Color reflectance of sediment core PS72/410-1. *PANGAEA.* https://doi.org/10.1594/PANGAEA.817614 (2013).

93. Kleman, J., Fastook, J., Ebert, K., Nilsson, J. & Caballero, R. Pre-LGM Northern Hemisphere ice sheet topography. *Clim. Past* **9**, 2365–2378 (2013).

94. Jakobsson, M. et al. The international bathymetric chart of the Arctic Ocean (IBCAO) Version 3.0. *Geophys. Res. Lett.* **39**, L12609 (2012).

Acknowledgements

Author contributions

K.J. developed the concept and led to the data interpretation and writing of the manuscript. K.S.W. and S.-I.N. proposed the study and led to the design of the analysis and interpretation and presentation of the results. J.-K.K. contributed to the textural and mineralogical analysis of the authigenic carbonates. All authors read and commented on the manuscript and contributed to the paper.

Competing interests

The authors declare no competing interests.

Additional information